University of BRISTOL

3SEP

R2S 2026 Preliminary Design Report

BristolSEDS Experimental Propulsion

RACE 2 SPACE

Bristol SEDS

Table of Contents

Note: BSEP is the propulsion arm of HyPower Bristol which is a subsidiary of BristolSEDS, the University of Bristol's Space Society. All 3 names can be used for the team interchangeably.

Part A

A1 – Project Introduction

This document is the Preliminary Design Report for BristolSEDS Experimental Propulsion (BSEP) Engine-4. Building upon the successful 5 kN design architecture established during the previous cycles, this year's mission aims to refine the system for higher performance. While the overarching goal remains a regeneratively cooled, additively manufactured engine producing 5kN of thrust, the 2026 mission introduces a significant technical leap with the team's first transition to Liquid Oxygen as the oxidizer.

Due to lessons learned during previous hotfire and integrated tests, the team has transitioned back to Inconel 718. With the ultimate goal of flying this Engine in the 9km liquid category at the European Rocketry Challenge (EuRoC) 2027, this material choice allows us to push the engine to its efficiency limits without having to worry about the fragility of Aluminium-based alloys in off-nominal scenarios that are inherently possible during integrated flight testing (such as ox-rich shutdowns).

The main innovation of this project lies in our shift to an "Ox-Centered Swirler" injector design. In a departure from previous fuel-centered architectures, this new design utilizes oxidizer injection through the central swirl element while fuel is injected through the outer stage. This configuration simplifies the manifold architecture, enhances mixing, and permits the removal of traditional film cooling to increase overall efficiency. New simulation methods will be developed to characterize and validate the novel swirler geometry as well as its effects on inner chamber wall thermals.

The R2S competition provides a platform to validate the performance of the engine and injector as well as give the team the opportunity to gain experience with cryogenics before moving towards a full launch vehicle.

A2 – Engine Design Overview

The BSEP Engine-4 is a high-efficiency, regeneratively cooled bi-propellant liquid rocket engine designed for a 5kN thrust target with an 8-second design burn time. The engine operates at a nominal chamber pressure of 20 bar using Liquid Oxygen (LOx) and Isopropyl Alcohol (IPA) as propellants.

The chamber is designed for additive manufacture using Inconel 718 to ensure maximum structural reliability under the extreme thermal loads of LOx combustion. Thermal management is primarily achieved through an opposite-flow regenerative cooling. IPA fuel circulates through 48 spiral cooling channels oriented at a 35° angle to the generatrix before reaching the injector plate.

The engine utilizes a co-axial swirl injector in an oxidizer-centred configuration. In this arrangement, LOx passes directly from the top of the engine into the inner swirlers, while the fuel enters the outer swirlers from the regenerative cooling channels.

The engine dimensions remain compatible with existing BSEP hardware to ensure seamless integration into existing launch vehicle systems and continues to allow all BSEP chamber and injectors to be interchangeable.

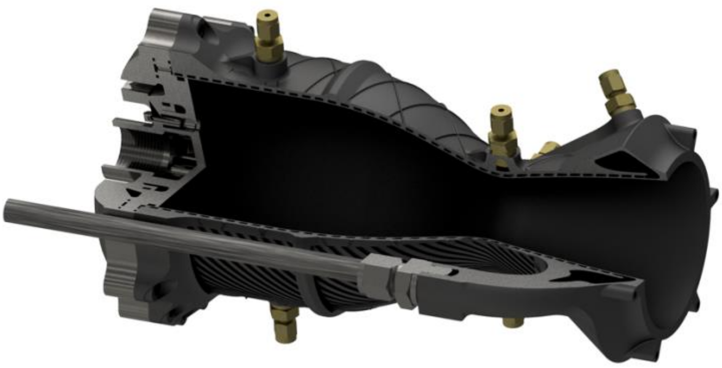

`

Figure 1, Quarter section view of full engine assembly CAD

A3 – Engine Parameter Table

Table 1: BSEP engine parameters

Parameter	Data	Unit
Propellants	IPA and LOx	n/a
Cooling Used	Regenerative, Film	n/a
Desired Fuel Mass Flow	0.864	kg/s
Desired Ox Mass Flow	1.296	kg/s
Port Connectors (Injector)	Ox: 3/4" BSPP	n/a
Port Connectors (Cooling)	Fuel: 1/2" BSPP (regen)	n/a
Design Thrust	5.0	kN
Design Burn Time	8.0	sec
Desired Fuel Delivery Pressure	30	bar
Desired Ox Delivery Pressure	30	bar
Designed Chamber Pressure	20	bar
Ignition System	Airborne Torch Igniter	n/a

A4 – Engine Description

A4.1 – Combustion Chamber

Figure 2, CAD render of Combustion Chamber

The combustion chamber shall be 3D printed out of Inconel 718. This material was chosen over an aluminium alloy such as CP1 (the material of BSEP's previous engine) due to its robustness and resistance to both cryogenic and high temperatures (exceeding 1000K). Moreover, the combination of the low melting point of aluminium and its vigorous reaction with liquid oxygen in cases of failure and hot spots meant it had to be eliminated from use within this engine due to the minimal margin of error afforded by these challenges. Overall, this decision was made to ensure the survival of the chamber if off-nominal conditions occur.

The chamber itself will have similar dimensions to BSEP's previous engines to maintain compatibility with previously manufactured items and ensure the possibility of integration within the currently owned launch vehicles. The chamber shall feature opposite flow regenerative cooling in the form of 48 spiral cooling channels at a 35° angle, film cooling, and additional cooling in hotspots through the effects of Polydimethylsiloxane (PDMS) added to the fuel mixture.

The robustness of this chamber will facilitate various component tests including the removal of film cooling capabilities from the injector to investigate the benefits to ISP, as mentioned within Section A4.2 – Injector.

A4.2 – Injector

Following our coaxial-swirl injector design from last year, we will be designing a further iteration, hoping to incorporate many new features, as well as lessons learned from the design of our previous injector. Working with LOx introduces a number of additional problems, both with respect to material compatibility, as well as sealing (which will be further discussed in A4.3 – Seals & Interfaces).

Since we are also using Liquid Oxygen this year it is necessary to switch back to using 316 Stainless Steel to manufacture the injector plate, rather than 6082 Aluminium. Following research into material compatibility we don't believe that the Aluminium would provide the requisite safety factor or not ignite or erode when at max temperature due to LOx exposure.

The primary difference between the new injector and its predecessor (excluding the change in Oxidizer) will be the use of "Ox Centred Swirlers", this is where the Oxidiser is injected into the combustion chamber through the central swirl element, whilst the Fuel is injected through the outer stage. This allows for the removal of film cooling from the engine, as the walls of the chamber are shielded from LOx impingement by the outer fuel stage, increasing efficiency and reducing complexity. Ox Centred Swirlers also simplify manifold design, as the Oxidizer entering from the top of the engine can be directly passed to the inner swirlers through a manifold, whilst the Fuel coming through the regen channels can enter a lower manifold to feed the outer swirlers. The differences between these two schemes can be seen in the figure below:

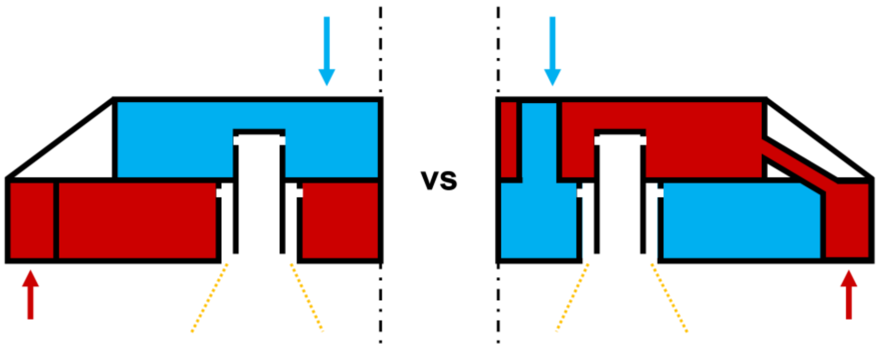

Figure 3 - A Comparison of Ox Centred (left) and Fuel Centred (right) Swirler Manifold Arrangements

The simplification of manifold design also results in fewer required seals, and much simpler manufacturing, especially when it comes to using CNC machines with fewer degrees of freedom.

However, the Ox Centred Swirlers are difficult to analyse since they cannot be characterised by Bazarov's analytical work. To ensure the procedures we use to design them are correct, we will be using StarCCM+ to simulate swirl injectors using water at low pressures. The same geometries will be tested in the lab to validate the simulations. With this validation complete we will move forward with the design of an Ox Centred Swirler design. If we cannot adequately characterise this behaviour, we are preparing an alternate (more conventional) design using Bazarov's equations for a Fuel Centred Swirler, which we have experience with from last year and is hence at a high TRL.

We shall again be endeavouring to reduce the number of inter-propellant seals, to enhance the safety of our engine, and incorporate all the sensing necessary to characterise the engine's performance. This can be seen in the image below.

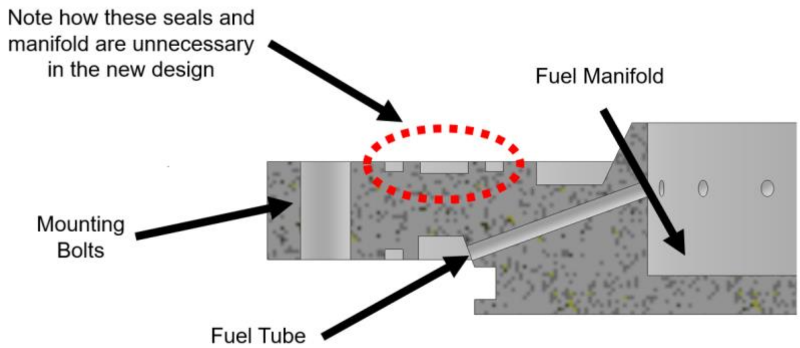

Figure 4: Cross Section of Preliminary CAD of the new Injector Plate

The figure (Figure 4) above displays the new design of the injector. It should be noted that due to the fuel manifold being next to the chamber, adding film cooling (if necessary) is very simple. More detailed renderings of the new injector plate can be found in B3.2 – Representative Design of This Year's Injector Plate.

A4.3 – Seals & Interfaces

As the engine is pre-chilled all the seals on it must be able to withstand cryogenic temperatures. There are a very limited number of materials that can operate in such harsh environments, prime amongst them is PTFE/PCTFE which has an operating temperature for O-Rings all the way down to around $-200\ °C$. The use of spring-energised seals may also be necessary for some piston/rod seals as PTFE is often too hard to form an effective sealing surface in these cases. These will be used as and when necessary, based on the design of the injector plate.

A5 – Project Timeline

The first milestone on our timeline is our single-swirler waterflow campaign where injector elements will be tested to validate the Ox-centered swirler design simulations. Following this, the chamber design is slated to be complete in February with the final injector design following in March.

Due to previous printing delays we've encountered, the goal is to begin the chamber print in March to leave a large amount of time for delays in the depowdering, CT scanning, and heat treatment processes, or any other issues that may arise. In April, the finalized injector design will be submitted to the University of Bristol machine shop for machining so by May all components are expected to be ready.

Table 2: BSEP Project timeline

Task	Jan	Feb	Mar	Apr	May	Jun	Jul
Single Swirler Waterflow	■						
Chamber Design Complete		■					
Injector Design Complete			■				
Chamber Sent for Printing			■				
Injector Sent for Machining				■			
All Seals and Consumables Ordered				■			
Chamber CT scan				■			
CDR deadline				■			
All Parts Received					■		
Fuel Assembly and Procedure Run-Through					■		
R2S hotfire							■
R2S symposium							■

A6 – Testing Plan Overview

The test outlines below are preliminary and subject to change following input from test facility and future potential design changes. Integration with the test facility at Airborne Engineering Ltd is facilitated by the ICD provided by the Race to Space competition.

A6.1 – Test 1: Full duration Burn 1

A full duration burn to act as a benchmark for thrust and chamber pressure. 8 seconds was chosen to put us at the EuRoC impulse limit and is the burn time we would use for a 9km launch vehicle.

Table 3: Test parameters for full duration burn hotfire

Property	Test Value	Unit
Oxidiser injector feed pressure	30	bar
Fuel injector feed pressure	30	bar
IPA mass flow	0.864	kg/s
LOx mass flow	1.296	kg/s
OF ratio	1.5	$(-)$
Chamber pressure	20	bar
Thrust	5	kN
Burn time	8	s
IPA consumed	6.912	kg
LOx consumed	10.368	kg

A6.2 – Test 2: Full duration Burn 2

A second burn to optimize from Test 1 and achieve the nominal values by increasing or decreasing mass flows and pressures as needed to achieve exactly 5kN of thrust.

A6.3 – Test 3: Depth of Throttle

A long burn starting at half throttle and gradually throttling down to determine the depth of throttle of the injector.

A6.4 – Test 4: Increased Chamber Pressure

Dependent on the thermal data results from Test 1 & 2, propellant feed pressures will be increased to test the limits of the engine's performance. Calculations will be able to be performed on the spot to confirm the engine could still survive the increased pressure with a 1.2× safety factor.

A7 – Planned Instrumentation

Multiple thermocouple ports are built into the chamber and pressure transducer ports are built into the injector to allow collection of sensor data. A series of wet and dry thermocouples are used to monitor the temperature of coolant along the channel walls, and a pair of pressure transducers are present on the injector to log the incoming pressure of the fuel and as well as the chamber pressure in the engine. The figure below lays out the sensor arrangement for the engine. From injector-face to nozzle, sensors are labelled based on their column and row. This allows for the unique labelling of each sensor when designating and data logging/graphing.

Table 3: Key instrumentation properties

Type	Value	Range	Part	Connection
Temperature	T(XX)	198 – 523 K	T type thermocouple	Type T Connection
Pressure	P(XX)	0 – 60 Bar	GPT200 Universal	4 pin M12

Figure 5: Instrumentation diagram

A8 – Design Calculations

A8.1 – Injector Sizing

Table 4: Injector geometry nomenclature

Variable	Definition
D_n	Diameter of the nozzle
R_s	Radius of the swirl chamber
r_{in}	Radius of the inlet to the swirl chamber
l_s	Length of the swirl chamber
l_n	Length of the nozzle
β	Angle of contraction of the inner wall

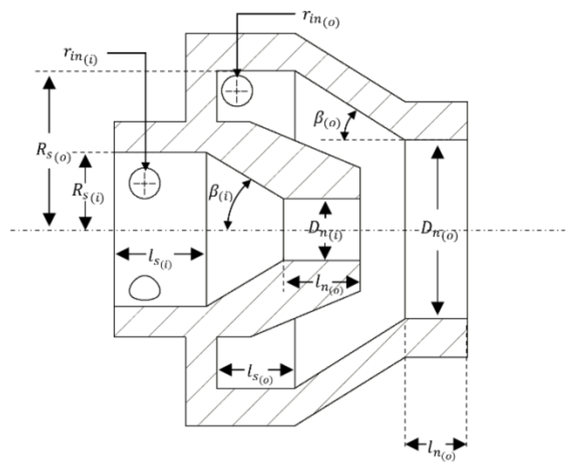

Using the methodology found in B3.1 – Swirl Element Sizing Method, and an in-house script to iterate it, we obtain the Oxidiser swirl element dimensions to be:

Table 5: Oxidiser swirl element properties & dimensions

Property	Value	Unit
Oxidiser mass flow	0.43	kgs^{-1}
Oxidiser nozzle diameter	6.8	mm
Oxidiser vortex chamber diameter	12	mm
Oxidiser Inlet Port Size	3	mm
Oxidiser Fan Angle	120	°

The fuel swirlers will be sized empirically thorough use of STARCCM+ simulation and Low-Pressure testing, as described in A4.2 – Injector.

A8.2 – Chamber Stress Calculations

A series of analytical and computational simulations were performed to validate the stress experienced by each part of the system.

A8.2.1 – Material Properties

The tabulated material properties detailed in Table 6 were provided by the material supplier and printing company, the MTC.

Table 6: Material properties of Inconel 718 used within chamber stress calculations

Property	Value	Units
Melting Point	1500	K
Maximum Operating Temp (MOT)	1050	K
Yield Strength	1172	MPa
Yield Strength at MOT	~758	MPa
Thermal Conductivity	18	$W/m \cdot k$
Thermal Conductivity at MOT	22.0	$W/m \cdot k$
Young's Modulus	208	GPa
Young's Modulus at MOT	130	GPa
Poisson Ratio	0.31	[--]
Thermal Expansion Coefficient	16.0×10^{-6}	$°C^{-1}$

A8.2.2 – Chamber Analysis

The stress results at every point along the engine contour were calculated using the equations in Appendix B3.3

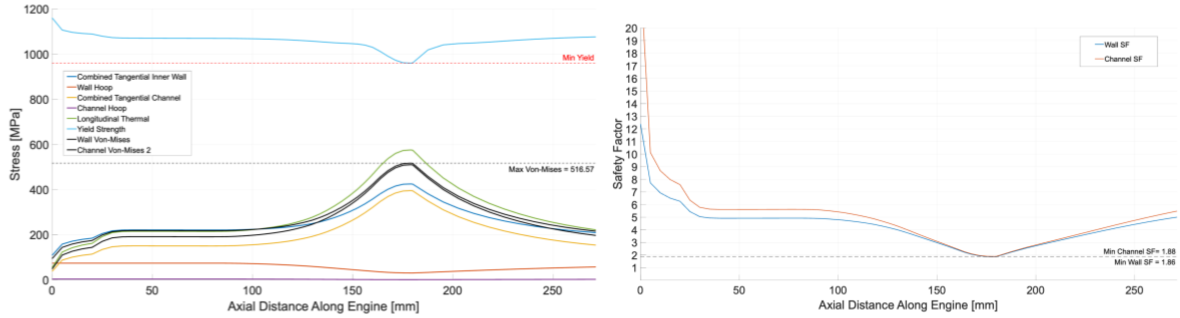

Figure 6: A graph of pressure and thermal stresses calculated (left) and their associated safety factors (right).

The tangential stresses were split into their hoop and thermal parts as well as combined. The yield strength values were extrapolated to accurately model when they will yield in each location at the operating temperature that location will experience. All stresses remain below the local Yield Strength; hence the engine will survive these stresses at steady-state.

Figure 5 displays the safety factor along the engine. At the most extreme thermal and stress conditions, i.e.: at the throat, the chamber still possess both a channel and wall safety factor exceeding 1.85, proving, in theory, that the chamber can be operated safely and with sufficient margin for error.

A8.2.4 – Stress Considerations

The above simulations demonstrate the "worst-case scenario" for the performance of the combustion chamber. Consideration should be given to the fact that the following beneficial factors have not been included in this modelling due to the difficulties involved in integrating these features:

- The Bartz equation has been used which is known to overestimate when compared to other sources such as the Levlev equation and empirical data.
- The effects of PDMS were not simulated. The addition of 1% PDMS to the fuel will act to considerably decrease wall temperatures at hotspots such as the throat and hence increase various material properties such as the tensile and yield strength.

As the analysis matures each of these features will be included, increasing the confidence in the stress and thermal simulations.

A8.3 – Bolt Calculations

A pattern of 12 M6 bolts has been included to secure the injector into the combustion chamber as well as to mount the chamber to the rocket itself. Half of the 12 bolts will be used for mounting the injector plate to the combustion chamber. From basic static equilibrium:

$$\sigma_b = \frac{P_c * A_I}{N_b * A_b} = \frac{20\ bar * \pi(0.0598)^2}{6 * 20.1 * 10^{-6}} = 186.3\ MPa \quad (1)$$

Where, σ_b is the stress on each bolt, P_c is the nominal chamber pressure, A_I is the circular area of the injector face exposed to the chamber pressure, N_b is the number of bolts exclusively in use to attach the chamber to the injector, and A_b is the tensile stress area of an M6 coarse pitch thread bolt. Considering a safety factor:

$$SF = \frac{\sigma_{yield\ of\ ISO\ Grade}}{\sigma_b}$$

With ISO Metric Bolt Grades of 4.6 and 10.9, the safety factors achieved are 1.29 and 5.05, respectively.

A8.4 – L-Bracket

Mounting is achieved using an aluminum mounting plate. This will transfer loads from the engine to the test stand. The same setup was proven highly effective in previous hot-fires of similar thrust. The full setup is seen below in Figure 7.

The engine mount, which interfaces with the test stand, is constructed out of 10mm plate aluminium with bolted interfaces for ease of assembly and disassembly. The L-bracket's structural performance was evaluated through Finite Element Analysis. A 5kN nominal thrust force was loaded at the contact surface between the engine mount and engine, assuming rigid bolt connections. This resulted in a maximum displacement and Von misses stress of 0.51mm and 52.52MPa respectively (safety factor of 5), indicating that the L-bracket can sustain loads substantially larger than the nominal design thrust.

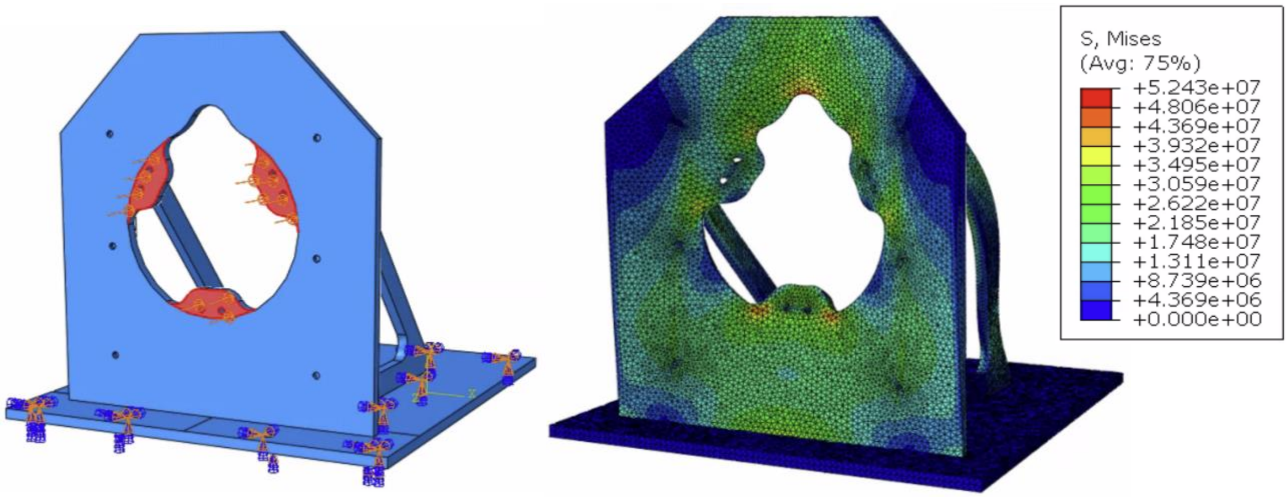

Figure 7: Finite Element Analysis of the L-bracket (deformation scale factor of 85).

The engine mount is to be fastened to the available thrust plate as specified by the Airborne Engineering Ltd J1 test site via 16xM10 and the BSEP engine via 6xM6 bolts. The bottom face mounting plate can be drilled to fit the requirements of the test stand in question.

8.4.1 – L-Bracket Bolt Calculations

Taking nominal thrust to be 5kN and given the maximum stress of the L-Bracket is 52.52MPa, the maximum shear stress per bolt on the bolts holding the L-Bracket to the thrust plate can be calculated using the following equation:

$$\tau_{bolt} = \frac{F_{engine}}{NA_{bolt}}$$

Here, τ_{bolt} is the maximum shear stress on a single bolt, F_{engine}, N is the number of bolts and A_{bolt} is the cross-sectional area of the bolt (assuming shear plane passes through the unthreaded shank). Evaluating this equation gives a maximum shear stress of 3.97MPa. This value can be compared to an existing bolt such as the 12.9 grade Socket Cap heads from Trident Racing Supplies, which has a shear strength of 517MPa. Therefore, we find that the bolts are sufficient to hold the L-bracket in place with a safety factor large enough to handle the added loads associated with a hardstart. Additionally, the thrust force will be distributed across the L-bracket so it is extremely unlikely that the bolts will experience the maximum stress, giving an added layer of confidence that the bolts are adequate.

8.4.2 – Engine Mount Bolts

The following bolt pattern was chosen to hold the engine in the mount:

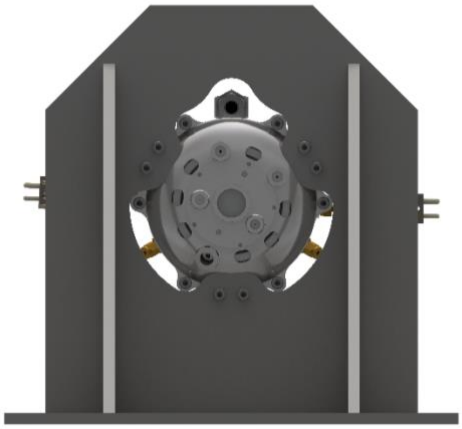

Figure 8: Bolthole locations within L-bracket

Three sets of two bolts were chosen to hold the engine in the L-bracket at equal intervals. Slots would also be cut to account for the pipes to attach to the mount. The bolts will go through the holes in the engine, injector plate and L-Bracket as shown in the top view CAD below:

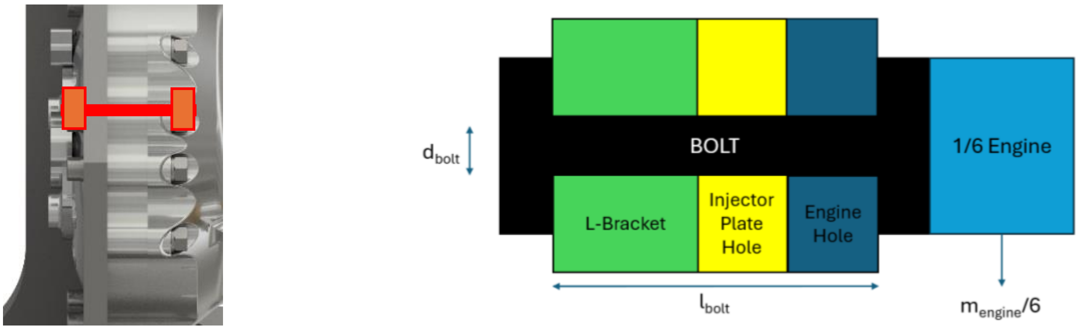

Figure 9: Bolt location highlighted on CAD (left). Schematic to describe assemble around bolt (right).

A8.5 – Chamber Thermal Analysis

Cooling strategies were converged upon though a series of thermal and mechanical stress simulations. Rocket Propulsion Analysis (RPA) was used to implement the Bartz equation for heat transfer coefficient through the chamber and nozzle boundary layer. Hot wall temperatures were then inserted into a thermal hoop stress calculation to derive stress values which fed redesign of thermal solutions until a final solution was converged upon. Additionally, a 10% film cooling solution was added to further reduce the thermals reached by the engine and a 1% addition of the additive PDMS will further reduce temperatures at hotspots. The percentage of PDMS used was chosen based upon the minimal heat flux reduction gains noticed past 1%, as displayed in **Error! Reference source not found.**.

PDMS reduces the total heat flux across the entire engine by creating silicon dioxide upon combustion which is deposited along the engine's inner walls and acts as an ablative thermal coating. At 1% PDMS, the expected heat flux reductions are within the range of 25-60% with negligible effects on the performance of the engine. When used in preliminary RPA simulations the PDMS additive will be modelled in the thermal analysis of the combustion chamber as approximately a 20% reduction in total heat flux at the throat. This will act as a conservative thermal estimate and may not accurately represent the potential heat flux reductions elsewhere in the engine.

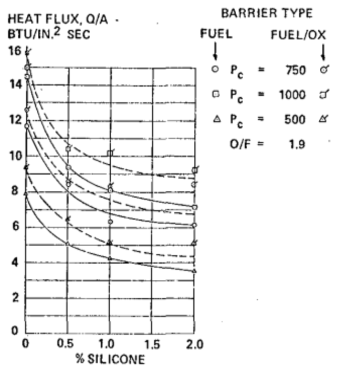

Figure 10: Heat flux reduction as a function of PDMS addition

Table 9: Chamber regenerative cooling channel geometry

Property	Value	Units
Wall thickness	0.8	mm
Rib thickness 'b' (Chamber – Throat - Manifold)	1.0 – 0.9 – 1.1	mm
Channel width 'a' (Chamber – Throat - Manifold)	4.0 – 2.0 – 3.0	mm
Channel height 'hc' (Chamber – Throat - Manifold)	2.0 – 2.0 – 2.0	mm
Angle to generatrix	35.0	$^\circ$

Table 10: Results of thermal simulations

Property	Value	Units
Maximum chamber-side wall temperature	933	K
Maximum coolant-side wall temperature	691	K
Maximum coolant temperature	381	K
Minimum velocity of coolant	3.88	ms^{-1}
Maximum heat flux	5437	kWm^{-2}
Increase in coolant temperature	83	K

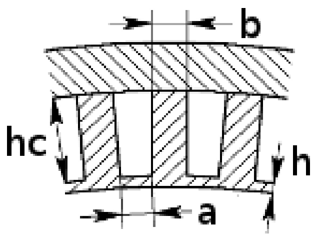

Figure 11: Cooling channel geometry

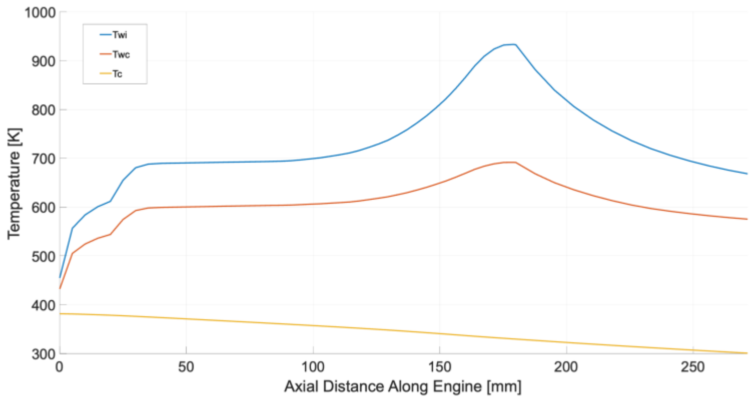

Figure 12: Chamber temperatures with respect to axial position (without PDMS addition)

The graph (Figure 12) and table above display the results of the thermal simulations without the simulated use of PDMS where Twi is the inner wall temperature chamber, Twc is the inner wall temperature of the cooling channels, and Tc is the temperature of the coolant. The graph demonstrates that even without factoring in the effects of PDMS the operating temperatures of the chamber are below the maximum recommend operating temperature of Inconel 718 (1050K) at all points along the engine.

A8.6 – Inlet Velocities

The inlet velocities for the Fuel and Oxidiser can be simply calculated using the flow rate equations:

$$Q = Av$$

Where Q is the volumetric flow rate, A is the cross-sectional area, and v is the average fluid velocity. We can rearrange this equation and substitute to obtain:

$$v = \frac{Q}{A} = \frac{\dot{m}}{A\rho}$$

Where ρ is the density of the fluid, and $\dot{m}$ is the mass flow rate.

We can therefore calculate the inlet velocities for the fuel and oxidiser ports using:

Table 7: Fuel and oxidiser inlet properties

Fluid	$\dot{m}\ (kg/s)$	A (m^2)	$\rho\ (kg/m^3)$	Velocity (ms^{-1})
IPA	0.86	6.9×10^{-5}	786	15.86
LOx	1.29	1.7×10^{-4}	1141	6.65

Part B

B1 – Positionality Statement

This year marks BristolSEDS Experimental Propulsion's 4th engine design and third entry into Race 2 Space. It builds upon BSEP's experience in liquid propulsion while incorporating new challenges for the team to face.

Engine-1 was originally designed for R2S 2024 by a small team of 5 members and was the University of Bristol's first every student built liquid rocket Engine. The design featured a 5kN regeneratively cooled AM Inconel 718 combustion chamber and a steel like-like impinging NOS/IPA injector. Due to a series of complications with the original print, the team was unable to test during the competition. With support from the Manufacturing Technologies Catapult, the team later received the chamber and were able to hotfire test the engine on January 10, 2025, at Airborne Engineering Ltd. Three successful tests were conducted, pushing the chamber 20% past its design thrust to 6kN, being the first student team in the UK to break 5kN of thrust and claiming the UK student thrust record at the time.

Engine-2 was designed for R2S 2025 and for HyPower's EuRoC '25 3km launch vehicle. This was a flight-weight iteration of Engine-1, utilizing CP-1 Aluminium for the combustion chamber and an aluminium coaxial swirl NOS/IPA injector plate. This was the first time the CP1 alloy had ever been used for a rocket engine. The engine was hotfired at R2S 2025, but due to swarf in the cooling channels introduced during post-machining, did not have a nominal burn. Because of the swarf clogging the fuel orifices, almost no IPA was able to flow through cooling channels and through the injector, removing the regenerative, film, and additive cooling effects from the PDMS. This complete lack of cooling caused the combustion chamber to fail in multiple locations. Nevertheless, this was an extremely interesting result and the team collected lots of data and lessons learned. The fact the engine fired under these conditions and achieved 2.1kN was a major success and validated the robustness of the swirler design. A steel H2/O2 torch ignitor was also tested at Astron Systems during R2S 2025, achieving 10 firings before melting.

Since the combustion chamber for Engine-2 was destroyed, the propulsion flight qualification campaign for HyPower's EuRoC '25 launch vehicle used Engine-1 instead. In September 2025, three integrated hotfires were successfully conducted at Astron System's facility using BSEP's SRAD feed system and tanks, qualifying the vehicle for flight and allowing the team to pass the Flight Readiness Review.

Engine-3 was designed as a replacement for the destroyed Engine-2, featuring an improved CP-1 chamber with spiral cooling channels which should decrease the inner wall temps by 10%. This engine will be used on HyPower's EuRoC 26' launched vehicle.

B2 – Mission Statement

Race 2 Space serves as an integral part of the test & development cycle for HyPower Bristol. HyPower Bristol has entered EuRoC yearly, competing in the liquid 3km category for 2024 and 2025. In 2026, we aim to launch a nitrous oxide and ethanol fuelled rocket to 9km. Without the facilities and expertise provided by Race 2 Space, the development and launch of a flight-optimised liquid rocket would be significantly more challenging.

Looking forward, the team is aiming to switch to a LOx based propellant rocket, also targeting 9km. This launch vehicle design will be primarily informed from data collected during R2S 2026 and will set the foundation for HyPower to aim for higher targets. Race 2 Space provides HyPower Bristol with a structured, repeatable environment to develop our propulsion system.

B3 – Appendices

B3.1 – Swirl Element Sizing Method

We use Bazarov's method from "Design and Dynamics of Jet and Swirl Injectors" to design elements which we are not simulating (i.e. the Ox Swirlers on this year's injector plate). This method follows:

Two pertinent design procedures are outlined by Bazarov: a single mono-propellant swirl injector (often referred to as a "simplex"), and the combination of two mono-propellant swirl injectors to form a coaxial swirl injector.

Single Swirler

1)

Prescribe the spray cone half angle (i.e. half the total fan angle), and determine both the geometric characteristic A and the flow coefficient μ from the plot:

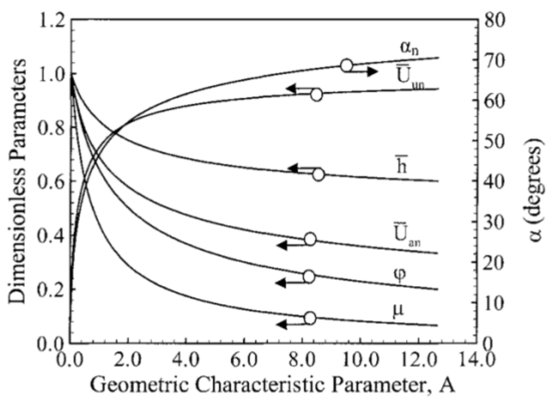

Figure 13 — Effects of A on other injector parameters

2)

Determine the nozzle radius using,

$$R_n = 0.475\sqrt{\frac{\dot{m}_i}{\mu\sqrt{\rho \Delta p_i}}}$$

3)

Specify the number of inlet passages (typically 2 to 4) and R_{in} from geometrical considerations, then the radius of the inlet passage is given by,

$$r_{in} = \sqrt{\frac{R_{in} R_n}{nA}}$$

Where R_{in} is the radial location of the center of the tangential channel, and n is the number of channels.

4)

Determine injector parameters based on the values calculated previously:

- Length of the tangential passages

$$l_{in} = (3\ to\ 6)\ r_{in}$$

- Nozzle length

$$l_n = (0.5\ to\ 2)\ R_n$$

- Vortex-chamber length

$$l_s > 2R_n$$

- Vortex-chamber radius

$$R_s = R_{in} + r_{in}$$

5)

We then find the Reynolds number of the inlet passages using:

$$Re_{in} = 0.637\frac{\dot{m}_i}{\sqrt{n} r_{in} \rho \nu}$$

Allowing us to calculate the friction coefficient:

$$\lambda = \frac{0.3164}{(Re_{in})^{0.25}}$$

6)

We can then find the equivalent area A_{eq} using the equation:

$$A_{eq} = \frac{R_{in} R_n}{n r_{in}^2 + \frac{\lambda}{2} R_{in}(R_{in} - R_n)}$$

Followed by using Figure 13 — Effects of A on other injector parameters) to determine μ_{eq} and α_{eq}.

7)

We can calculate the hydraulic-loss coefficient in the tangential passages using:

$$\xi = \xi_{in} + \lambda \frac{l_{in}}{2r_{in}}$$

Where ξ_{in} is determined from the plot of:

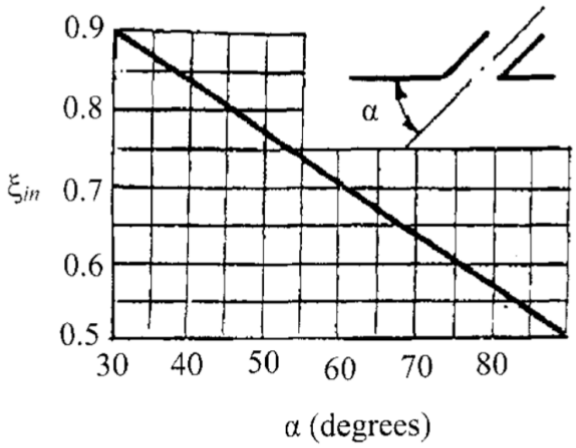

Figure 14 - Effect of tilt angle of injector passage on coefficient ξ_{in}

Where α (tilting angle of the tangential passage relative to the external surface of the vortex chamber) can be calculated using the equation:

$$\alpha = 90° - \tan^{-1}\frac{R_s}{l_{in}}$$

8)

The actual flow coefficient can then be determined using:

$$\mu_i = \frac{\mu_{eq}}{\sqrt{1 + \xi_i \mu_{eq}^2 \frac{A^2}{\bar{R}_{in}^2}}}$$

Where,

$$\bar{R}_{in} = \frac{R_{in}}{R_n}$$

9)

Which then allows us to obtain a new nozzle radius using the approximation:

$$R_n = 0.475\sqrt{\frac{\dot{m}_i}{\mu_i\sqrt{\rho \Delta p_i}}}$$

10)

Finally, we can calculate the geometric parameter A in the new approximation:

$$A^{(1)} = \frac{R_{in} R_n^{(1)}}{n r_{in}^2}$$

Steps 1-10 are then repeated until the calculated injector parameters converge.

B3.2 – Representative Design of This Year's Injector Plate

The following renders are of the injector plate which we tested at R2S 2025:

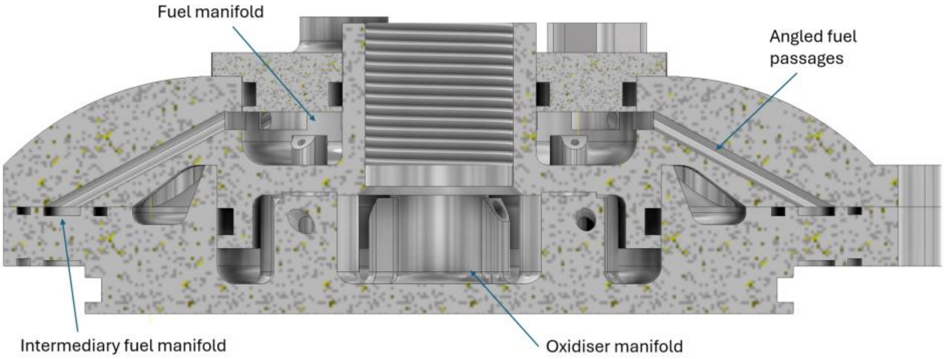

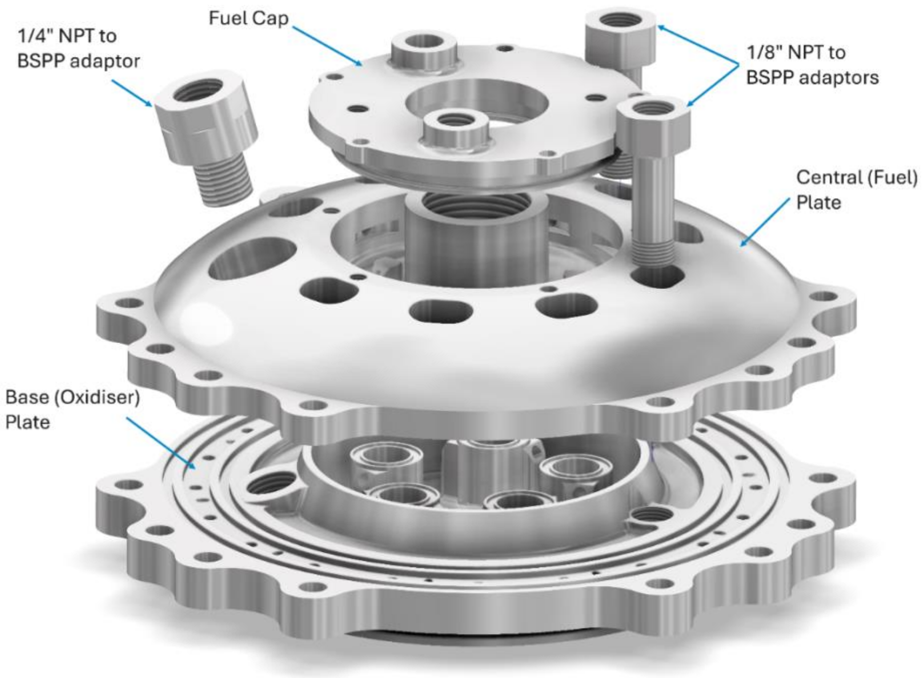

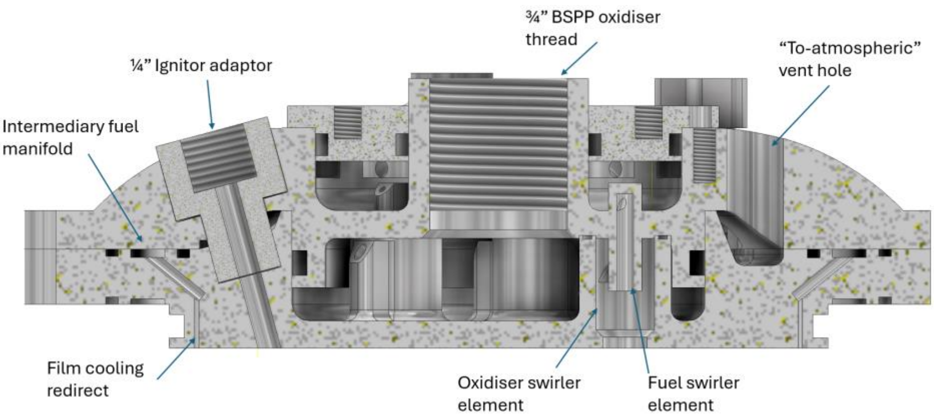

The new plate will look similar, with removal of the rounding as it adds machining time, and a relocation of the manifolds in accordance with the modified swirler arrangements. This can be seen in the preliminary CAD shown below – which despite not being in its final state, is representative of the direction the design will likely be heading in this year.

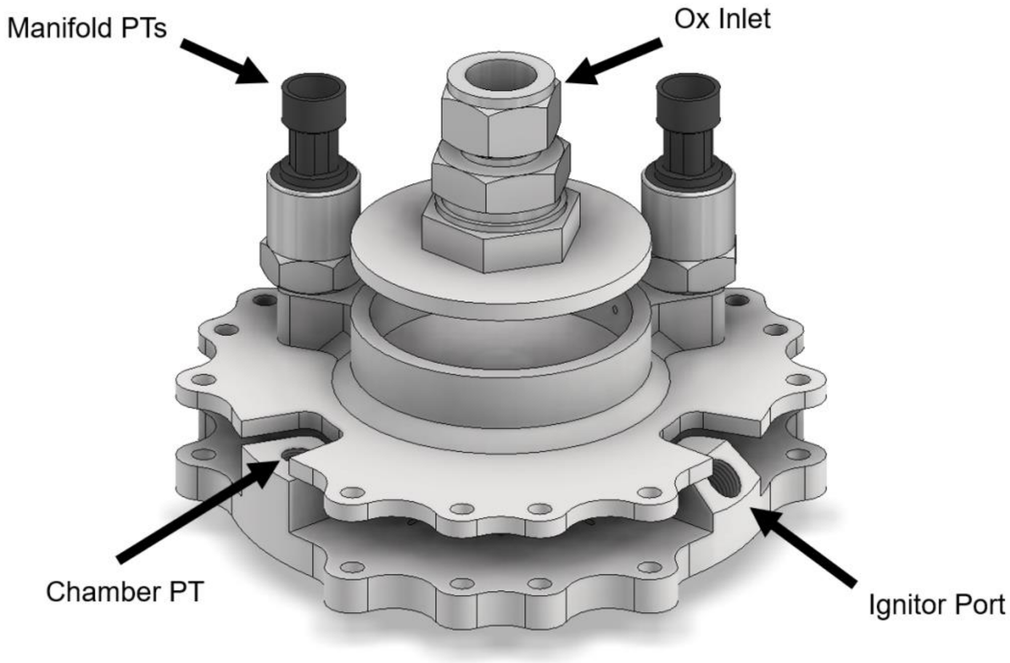

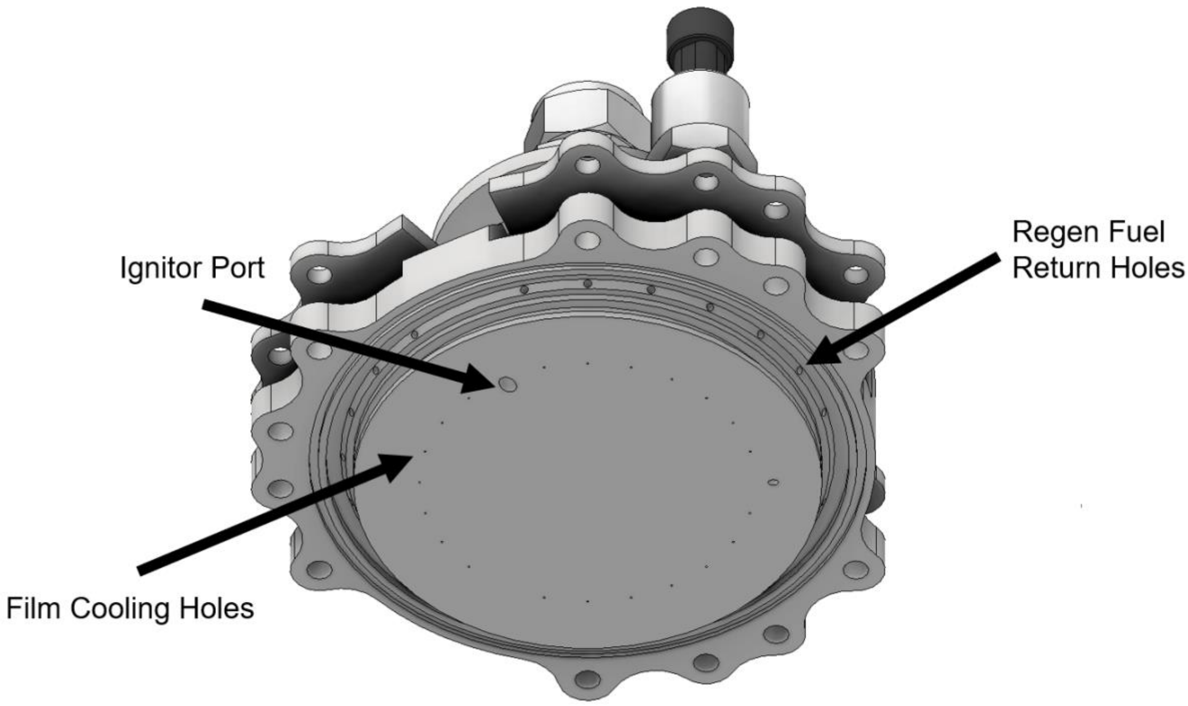

B3.3 – Chamber Stress Calculations

B3.3.1 – Hoop Stresses

A series of cases were looked at to determine the hoop stresses experienced by the engine. These simulations verify that the chamber and cooling channel walls will not burst under the pressures they will be subjected to.

Thick-Walled Hoop Stress

$$\sigma_\theta = \frac{P_a a^2 - P_b b^2}{b^2 - a^2} + \frac{a^2 b^2 (P_a - P_b)}{(b^2 - a^2) r^2}$$

Lame's equation for thick-walled hoop stress where σ_θ is the hoop stress, P_a is the pressure at the inner surface, P_b is the pressure at the outer surface, a is the inner diameter, b is the outer diameter, and r is the diameter inside the hoop at which the hoop stress is measured.

Multiple cases were tested with different combinations of the 20 bar chamber pressure, 30 bar coolant pressure and 1atm exterior pressure at different thicknesses of the material and point of the engine.

Table 8: Results for hoop stress calculations.

Position	Inner – Outer Pressure [bar]	Analytical Value [MPa]	Safety Factor (at MOT)
Chamber – Channel	20 – 30	77.8	9.7
Chamber – Wall	20 – 1 atm	24.4	31.0
Throat – Channel	20 – 30	33.8	22.4
Throat – Wall	20 – 1 atm	10.5	72.1
Chamber – Channel	1 atm – 30	224.0	3.3
Chamber – Channel	20 – 1 atm	150.0	5.1

Thin wall hoop stress was also used and found to give similar values.

B3.3.2 – Thermal Stresses

Multiple types of thermal stress equations were used as seen below to ensure no cracks or "doghouse effect," which will be described later, occur. Most of the equations were taken from Stephen D. Heister's "Rocket Propulsion."

Tangential Thermal Stress

Two equations were used to determine tangential thermal stress.

$$\sigma_{t1} = \frac{(P_{co} - P_g)D}{2t} + \frac{E\alpha q t}{2(1-v)k}$$

$$\sigma_{t2} = \frac{(P_{co} - P_g)}{2}\left(\frac{w}{t}\right)^2 + \frac{E\alpha q t}{2(1-v)k}$$

Where σ_t is the tangential stress, P_{co} is the coolant pressure, P_g is the combustion gas pressure, D is the chamber diameter, t is the inner wall thickness, E is the Young's Modulus, α is the thermal expansion coefficient, v is the Poisson's ratio, k is the thermal conductivity, and w is the internal width of the cooling channel. Tangential stresses are created by the internal pressure in the coolant passage and its relationship to the local gas pressure as well as due to thermal growth of the material on the heated side of the passage The first half of both equation takes into account the hoop stresses, the first equation calculating it for the inner wall and the second for the channels. The second half of the equation represents the tangential thermal stress induced by heat transfer.

Longitudinal Thermal Stress

$$\sigma_l = E\alpha(T_w - T_{ow})$$

Where σ_l is the longitudinal stress, T_w is the hot wall temperature, and T_{ow} is the cold wall temperature. The longitudinal stresses result from the tendency of the heated side of the passages to grow in length.

Thermal Buckling Stress

$$\sigma_b = \frac{EE_c\frac{t}{D}}{(\sqrt{E}+\sqrt{E_c})^2\sqrt{3(1-v^2)}}$$

Where σ_b is the buckling stress and E_c is the compression modulus.

B3.4 – L-Bracket Drawing

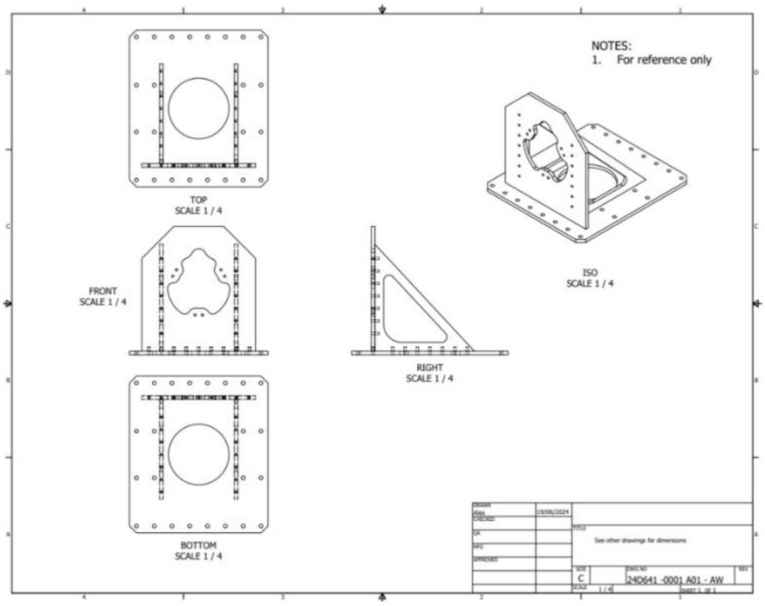

Figure 15, Drawings for fabrication of L-bracket used to support engine during testing.

B3.5 – Engine Mount Bolt Calculations

To verify if bolts will be suitable to hold the engine in place before ignition, a calculation was made with the following simplified diagram, where “1/6 Engine” is a sixth of the lumped mass on the end of a single bolt, since there are six bolts to distribute the load.

Then we can use the bearing stress equation to approximate the load on the bolt:

$$\sigma_{bearing,bolt} = \frac{m_{engine}}{6d_{bolt}l_{bolt}}$$

Assuming the engine mass is 6kg, this will give the bearing stress of 3.7KPa (2.s.f). Compared to the Trident Racing bolt, which has a tensile strength of 1206MPa (Trident Racing Supplies, n.d.), this design would be sufficient. In reality, there would be distributed load along the bolt with considerably more force at the bottom of the bolt towards the engine and the top of the bolt towards on the other side. However, given that the bearing stress is several orders of magnitude below the yield strength, we can conclude it is not necessary to evaluate this stress distribution.